The influence of acute unloading on left ventricular strain and strain rate by speckle tracking echocardiography in a porcine model

Geir Olav Dahle,[1,2] **Lodve Stangeland,**[2] **Christian Arvei Moen,**[2] **Pirjo-Riitta Salminen,**[1,2]
Rune Haaverstad,[1,2] **Knut Matre,**[2] **and Ketil Grong**[2]

[1]*Section of Cardiothoracic Surgery, Department of Heart Disease, Haukeland University Hospital, Bergen, Norway; and*
[2]*Department of Clinical Science, University of Bergen, Bergen, Norway*

Dahle GO, Stangeland L, Moen CA, Salminen PR, Haaverstad R, Matre K, Grong K. The influence of acute unloading on left ventricular strain and strain rate by speckle tracking echocardiography in a porcine model. *Am J Physiol Heart Circ Physiol* 310: H1330–H1339, 2016. First published March 11, 2016; doi:10.1152/ajpheart.00947.2015.—Noninvasive measurements of myocardial strain and strain rate by speckle tracking echocardiography correlate to cardiac contractile state but also to load, which may weaken their value as indices of inotropy. In a porcine model, we investigated the influence of acute dynamic preload reductions on left ventricular strain and strain rate and their relation to the pressure-conductance catheter-derived preload recruitable stroke work (PRSW) and peak positive first derivative of left ventricular pressure (LV-dP/dt_{max}). Speckle tracking strain and strain rate in the longitudinal, circumferential, and radial directions were measured during acute dynamic reductions of end-diastolic volume during three different myocardial inotropic states. Both strain and strain rate were sensitive to unloading of the left ventricle ($P < 0.001$), but the load dependency for strain rate was modest compared with strain. Changes in longitudinal and circumferential strain correlated more strongly to changes in end-diastolic volume ($r = -0.86$ and $r = -0.72$) than did radial strain ($r = 0.35$). Longitudinal, circumferential, and radial strain significantly correlated with LV-dP/dt_{max} ($r = -0.53$, $r = -0.46$, and $r = 0.86$), whereas only radial strain correlated with PRSW ($r = 0.55$). Strain rate in the longitudinal, circumferential and radial direction significantly correlated with both PRSW ($r = -0.64$, $r = -0.58$, and $r = 0.74$) and LV-dP/dt_{max} ($r = -0.95$, $r = -0.70$, and $r = 0.85$). In conclusion, the speckle tracking echocardiography-derived strain rate is more robust to dynamic ventricular unloading than strain. Longitudinal and circumferential strain could not predict load-independent contractility. Strain rates, and especially in the radial direction, are good predictors of preload-independent inotropic markers derived from conductance catheter.

speckle tracking echocardiography; strain; strain rate; acute left ventricular unloading; contractility

---

NEW & NOTEWORTHY

In a porcine model, we demonstrate that strain rate derived by speckle tracking is more resistant to acute dynamic preload reductions than strain in longitudinal, circumferential, and radial echocardiographic planes. Strain rate is also the best parameter describing the load-independent contractility markers preload recruitable stroke work (PRSW) and dP/dt_{max}.

CONTRACTILITY IS AN IMPORTANT entity when describing cardiac function. However, because of the interplay with the Frank-Starling mechanism, contractility has proven especially diffi-

cult to measure. Intraventricular pressure volume analysis during acute loading manipulation is often regarded the gold standard to quantify load-independent contractility (6). These parameters require highly invasive measurements and are thus rarely available in a clinical setting. As such, noninvasive estimates of contractile function are warranted both in clinical and experimental settings.

Echocardiographic recordings enable myocardial deformation to be measured and quantified as strain and strain rate (11). However, these measurements will not reflect true contractility as they are also influenced by factors such as heart rate, ventricular geometry, loading conditions, and tissue compliance. The effects of preload and afterload on deformation measurements have been investigated in several studies, especially with tissue Doppler imaging (TDI)-derived deformation. By mathematically modeling in vitro and in vivo these studies investigate regional myocardial deformation under different steady-state conditions (1, 2, 7, 13, 24, 29, 30). There is an agreement that these indexes of systolic left ventricular function are load dependent but to what degree is more uncertain.

In a clinical setting, speckle tracking echocardiography (STE) is by many the preferred method for measuring myocardial deformation, especially for the assessment of global systolic function. Compared with TDI, this method is more automated and avoids the well-known errors of angle dependency and noise-related issues. However, STE also has limitations, the most important related to frame rate of the B-mode recordings.

During steady-state conditions, previous studies have compared both TDI and STE with pressure-volume loops (18, 25, 31). Also, regional TDI-derived tissue velocities and strain have been examined during acute dynamic preload reductions (1). To our knowledge, no study has undertaken a direct beat to beat comparison between STE-derived strain and strain rate and acute preload manipulation at different contractile states.

We hypothesized that STE-derived strain and strain rate can be used to evaluate left ventricular load-independent contractility. Therefore, this study was designed to investigate how global STE strain and strain rate are affected by acute dynamic ventricular unloading caused by caval occlusions. Also, the relationship between STE strain and strain rate and the invasive contractility parameters preload recruitable stroke work (PRSW) and peak positive of the first derivative of left ventricular pressure (LV-dP/dt_{max}), obtained from a pressure-conductance catheter, was evaluated.

MATERIALS AND METHODS

Experiments were performed in seven pigs weighing 41 ± 2 kg (SD) of either sex. All procedures were performed in accordance with

Address for reprint requests and other correspondence: G. O. Dahle, Dept. of Clinical Science, Univ. of Bergen, Haukeland Univ. Hospital, N5021 Bergen, Norway (e-mail: geir.olav.dahle@helse-bergen.no).

http://www.ajpheart.org

international guidelines described in the European Communities Council Directive of 2010 (63/EU). The experimental protocol was approved by the Norwegian State Commission for Laboratory Animals (Project No. 20113923).

Anesthesia and surgical preparation. Animals were acclimatized for at least 7 days. The night before experiments, they fasted with ad libitum access to water. Premedications with ketamine (20 mg/kg), diazepam (10 mg), and atropine (1 mg) were given as an intramuscular injection in the neck. Anesthesia was induced by spontaneous mask ventilation with isoflurane and oxygen. Two ear veins were cannulated allowing maintenance of anesthesia with loading doses and continuous infusions of pentobarbital (15 mg/kg and 4 mg·kg^{-1}·h^{-1}), midazolam (0.3 mg/kg and 0.3 mg·kg^{-1}·h^{-1}), fentanyl (0.02 mg/kg and 0.02 mg·kg^{-1}·h^{-1}), and vecuronium (0.6 mg/kg and 0.3 mg·kg^{-1}·h^{-1}). Animals were intubated via a tracheostomy and volume controlled positive pressure ventilation commenced with tidal volumes set to 11 ml/kg (Julian; Dräger, Lübeck, Germany). A mixture of oxygen and 57% nitrous oxide was used and end tidal carbon dioxide was kept between 5.0 and 5.7 kPa by adjustment of respiratory rate. A more detailed description of the anesthetic protocol and justification for the safe usage of muscular relaxants can be found elsewhere (12, 15). The bladder was drained through a suprapubic catheter. A balloon occlusion catheter was placed in the proximal inferior caval vein via the right femoral vein, allowing repeated preload reduction sequences. A retrograde pressure-conductance catheter was advanced into the left ventricle through the left external carotid artery and connected to a conductance signal conditioner (Sigma M; CDLeycom, Hengelo, The Netherlands). Proper placement was confirmed by echocardiography (Vivid E9; GE Vingmed Ultrasound, Horten, Norway). Also, segmental conductance signals displaying paradox movements, indicating aortic sampling, were excluded. Aortic pressure was monitored by a pressure-tip catheter (MPC-500; Millar, Houston, TX) placed in the aortic arch through the right external carotid artery. The right external jugular vein was used to advance a Swan Ganz catheter (139H-7.5F; Edward Lifesciences, Irvine, CA) to the pulmonary artery to obtain cardiac output (Vigilance II; Edward Lifesciences).

An acoustic window measuring about 8 × 6 cm was made by careful surgical resection of part of the chest wall in the median line cranial to the xiphoid process, carefully keeping the pericardium and pleura intact. This window was filled with ultrasonic gel to achieve sufficient ultrasound probe offset to record the entire left ventricle.

Echocardiographic and pressure conductance recordings. Both echocardiography and pressure conductance loops were recorded simultaneously. Each run started with a sequence of 6–10 stable beats followed by 6–12 beats of acute dynamic preload reductions achieved by rapid inflation of the balloon in the proximal inferior caval vein using a syringe. All recordings were done during respirator shut-off in end expiration. Aortic pressure signal together with a common ECG was connected to the auxiliary channel on both the conductance signal conditioning unit and the ultrasound scanner. At the beginning of each recording a spike in the aortic pressure signal was created by briefly switching the pressure control unit (TC-510; Millar) off and on. This spike was used as a common identifier allowing the echocardiographic recordings to be matched in time with their respective pressure volume loops.

Echocardiography was performed with a 6-MHz cardiac probe (6S; GE Vingmed Ultrasound). Imagery during dynamic preload reductions was obtained for both long axis and short axis. The long-axis B-mode cineloops were obtained in a standard, apical four chamber view. The short axis was obtained at approximately mid-left ventricle. Since the pig has large papillary muscles, the recorded plane is slightly below the standard plane described in the current human guidelines for chamber quantification by echocardiography, which is above the papillary muscles (20). Consistency was assured by carefully adjusting the short-axis plane to obtain a circular short axis of the homogenous contracting left ventricle and just cutting the top of the

papillary muscles (Fig. 1). Each recording was optimized with respect to frame rate and resolution by selecting minimum sector depth and width while still being able to depict the entire left ventricular wall throughout the cardiac cycle in the two recorded views. With these settings, the resulting average frame rate for all recordings was 103 ± 11 fps (SD). To avoid excessive depth in the apical image settings, the probe was continuously lowered as the heart emptied during unloading. However, no direct contact between probe and pericardium was allowed.

Three inotropic states were examined: Baseline and continuous dobutamine infusions at two rates: Dob$_{low}$ (5–10 μg·kg^{-1}·min^{-1}) and Dob$_{high}$ (7.5–12.5 μg·kg^{-1}·min^{-1}). The dobutamine infusion rates were adjusted in each pig targeting a stable LV-dP/dt_{max} increase of ~50 and 100% compared with baseline value. The new inotropic state was reached when LV-dP/dt_{max} and cardiac output had reached a new plateau and stabilized for 5 min.

During the infusion of dobutamine, the hemodynamic variations were more pronounced and there were more tendencies for arrhythmias, often forcing repeated caval occlusion runs. Parallel conductance estimates with saline injections were measured at each inotropic state after the echocardiographic protocol was completed.

Data analysis. All speckle tracking was performed with commercial software (EchoPac BT12; GE Vingmed Ultrasound). Trackings were accepted when both automatic and visual tracking were acceptable for all segments. Drift compensation was enabled, and all smoothing parameters were kept in default position (21). End of diastole was defined as the first deflection of the QRS-complex in the ECG. With the use of this set point, the time to aortic valve closure was measured from a pulsed wave Doppler recording in the left ventricular outflow tract and used to define the end of systole. In addition to a visual confirmation of a similar ECG pattern and heart rate, this time measurement was acquired immediately before the four chamber and short-axis recordings. Longitudinal, circumferential, and radial peak systolic strain and strain rate were reported as the average of all six segments in the respective direction. Strain and strain rate curves with respective ECG and timing signals were exported to an in-house developed software (MATLAB; MathWorks, Natick, MA) for synchronization with pressure volume data.

All pressure-conductance data were exported to another in-house developed software (MATLAB; MathWorks) where analysis was performed. Parallel conductance, calculated by the hypertonic saline bolus method at the end of each inotropic level, was subtracted from conductance signals (5). Just before unloading, 6–10 beats were used to calculate the stable hemodynamic indices. Stable stroke volumes were calibrated for continuous cardiac output measurement acquired just before the pressure-volume-loop acquisitions. The consecutive beats during the unloading by caval occlusion were used to calculate PRSW and end-systolic- and end-diastolic pressure-volume relations (ESPVR and EDPVR) (6, 14). Volumes were normalized for body surface area (16). The isovolumic relaxation constant, τ, was calculated according to Raff and Glantz (22). The slope of the PRSW and the LV-dP/dt_{max} were chosen as the main references for inotropic state.

For all cardiac cycles, peak systolic strain and strain rate were paired to their corresponding end-diastolic volume (EDV). Both strain/strain rate and corresponding EDVs were subtracted from their respective mean value from each individual caval occlusion. The data from all situations were then plotted in a common scatterplot, passing through the origin (mean values). Statistically this will be identical to combining a grand mean of the individual slopes, eliminating the noise from uncertainty in timing and parallel conductance.

At least 6 mo after the original analysis, 20 short-axis and 20 long-axis beats were randomly selected from the dataset and reanalyzed by the same observer (G. O. Dahle) for assessment of intraobserver variability. The same selection of beats was also analyzed by another observer (C. A. Moen) for interobserver variability assessment.
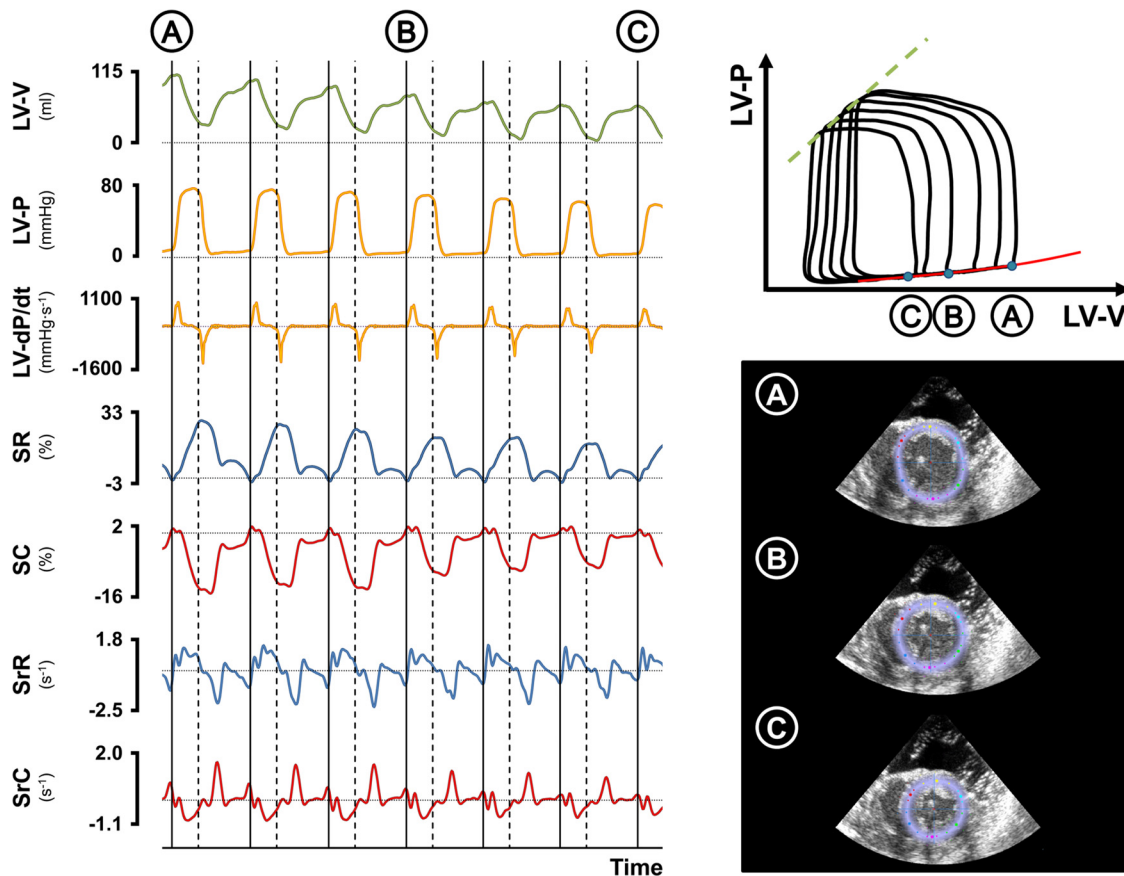
Fig. 1. Typical waveforms from conductance catheter and echocardiographic speckle tracking (*left*) during an acute dynamic preload reduction with end-diastole (solid lines) and end-systole (dashed lines), corresponding pressure volume loops (*top right*) with end-systolic pressure-volume relation (dashed green line) and logarithmic end-diastolic pressure-volume relation (solid red line), and short-axis B-mode images at end-diastolic frame (*bottom right*) with overlayed speckle tracking-derived circumferential strain estimate. *A*, *B*, and *C*: corresponding times. LV, left ventricle; V, volume; P, pressure; dP/dt, the 1st derivative of pressure; SR, radial strain; SC, circumferential strain; SrR, radial strain rate; SrC, circumferential strain rate.

Statistics. Statistical analysis was performed with commercial software (SigmaStat 3.5; Systat Software). All hemodynamic data were found to be normal and equally distributed by Kolmogorov-Smirnov and the Levene's median tests, respectively ($P \geq 0.05$ for both). Repeated measurement one-way ANOVA was used to test the effect of dobutamine infusions. Student-Newman-Keul's tests were used to compare individual means in case of a significant ANOVA. The method of least square approach was used in the linear regression analyses. For intra- and interobserver variability, the coefficient of variation and intraclass correlation coefficient were calculated. Values are presented as mean ± SE unless otherwise noted and $P < 0.05$ was considered significant.

RESULTS

Effect of dobutamine infusion on cardiac performance. Both the main inotropic markers, LV-dP/dt_{max} and PRSW, differed significantly between each situation indicating different contractile states (Table 1). Furthermore, the ESPVR increased during dobutamine infusions ($P = 0.014$) but was not statistically significant between baseline and Dob$_{low}$. Similar changes were seen for cardiac index ($P = 0.029$), but in addition to increased inotropy, this difference was also caused by a corresponding increase in heart rate ($P = 0.005$). Isovolumic relaxation was enhanced with increasing dobutamine doses as indicated by a more negative LV-dP/dt_{min} and reduced τ ($P = 0.002$ and $P < 0.001$). No significant changes were seen in

intraventricular volumes and pressures. All strain and strain rate parameters were enhanced with high dobutamine infusions (Dob$_{high}$) except for longitudinal strain, which only displayed a borderline significance ($P = 0.07$). Contrast analysis demonstrated no statistically significant differences for strain and strain rate values between baseline and Dob$_{low}$.

Dynamic preload reduction and STE-derived parameters. STE-derived parameters were paired with respective EDV from all beats from caval occlusion runs resulting in a total of 205 and 200 data pairs for the short-axis and long-axis recordings, respectively. Load alterations correlated to changes in deformation for all parameters ($P < 0.001$ for all), but the correlation was especially strong for longitudinal and circumferential strain ($r = -0.86$ and $r = -0.72$; Fig. 2, *A* and *C*) compared with radial strain ($r = 0.35$; Fig. 2*E*). Circumferential strain rate was the variable with the weakest correlation to loading alterations ($r = 0.25$; Fig. 2*D*), whereas stronger correlations were found for longitudinal and radial strain rates ($r = -0.40$ and $r = -0.35$; Fig. 2, *B* and *F*).

PRSW-, LV-dPdt_{max}-, and STE-derived parameters. Three contractile states in each of the 7 animals totaling 21 measurements of strain and strain rate in all directions are plotted vs. PRSW and LV-dPdt_{max} (Figs. 3, 4, and 5). Strain rate correlated significantly in all planes against PRSW in contrast to strain where the correlation was significant in the radial direc-

Table 1. *Left ventricular variables at baseline, low, and high levels of inotropic stimulation with dobutamine*

Variable	Baseline (A)	Dob$_{low}$ (B)	Dob$_{high}$ (C)	RM-ANOVA
HR, beat/min	94 ± 6	100 ± 6	116 ± 8[a,b]	$P = 0.005$
LV-SP$_{max}$, mmHg	108 ± 5	116 ± 8	117 ± 6	$P = 0.18$
LV-EDP, mmHg	12.1 ± 1.3	12.8 ± 1.4	11.8 ± 1.1	$P = 0.44$
LV-dP/dt_{max}, mmHg/s	1,388 ± 58	2,426 ± 264[a]	3,548 ± 1171[a,b]	$P < 0.001$
LV-dP/dt_{min}, mmHg/s	−2,489 ± 113	−3140 ± 291[a]	−3,514 ± 305[a]	$P = 0.002$
τ, ms	31.5 ± 0.7	25.4 ± 1.6[a]	20.6 ± 1.4[a,b]	$P < 0.001$
CI, l·min^{-1}·m^{-2}	4.2 ± 0.3	5.0 ± 0.4	5.8 ± 0.5[a]	$P = 0.029$
LV-EDV$_i$, ml/m^2	79 ± 5	89 ± 10	85 ± 9	$P = 0.59$
LV-ESV$_i$, ml/m^2	34 ± 4	38 ± 7	36 ± 5	$P = 0.65$
SV$_i$, ml/m^2	46 ± 4	51 ± 5	50 ± 5	$P = 0.64$
LV-EF, %	58 ± 4	59 ± 5	60 ± 4	$P = 0.69$
LV-SW$_i$, mmHg·ml·m^{-2}	4,278 ± 257	5,380 ± 762	5,623 ± 763	$P = 0.16$
ESPVR, mmHg/ml	1.2 ± 0.2	1.6 ± 0.2	2.5 ± 0.3[a,b]	$P = 0.014$
PRSW, mmHg	54 ± 6	71 ± 5[a]	88 ± 4[a,b]	$P = 0.002$
β, unitless	0.027 ± 0.004	0.027 ± 0.003	0.028 ± 0.003	$P = 0.90$
Longitudinal strain, %	−11.8 ± 0.9	−13.7 ± 1.6	−15.1 ± 1.5	$P = 0.07$
Longitudinal stain rate, 1/s	−1.12 ± 0.04	−1.45 ± 0.14	−2.23 ± 0.19[a,b]	$P < 0.001$
Circumferential strain, %	−11.8 ± 0.7	−13.8 ± 1.1	−15.1 ± 1.4[a]	$P = 0.041$
Circumferential strain rate, 1/s	−1.04 ± 0.05	−1.29 ± 0.07	−1.73 ± 0.14[a,b]	$P < 0.001$
Radial strain, %	36.4 ± 2.9	46.6 ± 4.3	55.8 ± 6.4[a]	$P = 0.019$
Radial strain rate, 1/s	2.44 ± 0.12	3.24 ± 0.15	5.09 ± 0.44[a,b]	$P < 0.001$

Values are mean ± SE ($n = 7$). Dob$_{low}$ and Dob$_{high}$, low and high levels of inotropic stimulation with dobutamine; LV, left ventricle; subscript i, value indexed for body surface area; HR, heart rate; SP$_{max}$, peak systolic pressure; EDP, end-diastolic pressure; dP/dt_{max} and dP/dt_{min}, maximum and minimum of the first derivative of pressure; τ, left ventricular isovolumic relaxation time constant (Glantz); CI, cardiac index; EDV and ESV, end-diastolic and end-systolic volumes; SV, stroke volume; EF, ejection fraction; SW, stroke work; ESPVR, slope of end-systolic pressure volume relationship; PRSW, slope of preload recruitable stroke work; β, slope of logarithmic fitted end-diastolic pressure volume relationship. P values are for one-way analysis of variance for repeated-measurement (RM)-ANOVA. Lowercase superscript letters denote significant difference from value(s) in columns with corresponding uppercase letters by post hoc multiple contrasts.

tion only ($P = 0.010$; Fig. 5A). The best correlation to PRSW was radial strain rate ($r = 0.74$; Fig. 5B). All STE parameters correlated to LV-dPdt_{max}, strain rate in all directions had stronger and more significant correlations then their respective strain parameters.

DISCUSSION

Load dependency of strain and strain rate. In this study, the correlations with preload variations were stronger for strain than for strain rate in both the longitudinal and circumferential directions (Fig. 2). In addition, the slope relative to the measured values is three to four times steeper per volume unit for strain than for strain rate. This demonstrates that strain is more preload dependent than strain rate in these directions. This is also reflected in the lack of a significant correlation between both longitudinal and circumferential strain vs. the load-independent measure of contractility PRSW, as opposed to the corresponding strain rate values (Figs. 3 and 4). For LV-dP/dt_{max}, a more load sensitive measure of inotropy (9), both strain and strain rate parameters correlate; strain rate better than strain. Thus the load dependency of strain limits its ability to predict true inotropic function. For the radial direction both the correlation and the magnitude of the slope relative to changes in EDV are similar but less pronounced for both strain and strain rate (Fig. 2). Furthermore, there are significant correlations between radial strain and strain rate and both PRSW and LV-dP/dt_{max}, but also in this direction, strain rate reflects load-independent contractility better than strain (Fig. 5). Our findings with load dependency of STE-derived strain and strain rate are in accordance with previous studies using other evaluation methods (29, 30).

When altering loading conditions pharmacologically or by fluid manipulation in vivo, a fundamental methodological

problem is the inevitable triggering of several cardiac reflexes influencing contractility. In other words, the magnitude of strain and strain rate changes in these studies do not reflect load dependency per se, but the total effect of the loading interventions including the responses in the cardiovascular system. This may explain contradictory results in a clinical setting (3, 30). This problem was recognized in a previous study using left ventricular EDP, arterial elastance, left ventricular myocardial volume, and PRSW in a multiple regression analysis model to predict TDI-derived circumferential and radial strain and strain rate in a chronic murine model (13). This study demonstrates that strain rate in both directions is highly correlated to PRSW. However, in contrast to the results in the present study, none of the strain or strain rate values significantly correlated with the preload marker EDP. Notably, the relative statistical variance in EDP in the referred study was quite large and differences in filling time and diastolic compliance between mouse and pig hearts may explain some of this difference.

The present study aimed at isolating load from contractility by measuring only the first 8–10 beats of an acute dynamic preload reduction. This should precede the neuro-humoral feedback mechanisms as well as the Bowditch and Anrep effects and therefore keep the inotropic state of the myocardium unaltered (10, 19). In principle, our findings reflect the true influence of load alteration by caval occlusion on the strain and strain rate values. As heart rate and contractility remain unaltered, this should include geometrical changes and load changes, only.

In a similar protocol, myocardial strain and velocities by TDI in longitudinal and radial directions were compared with conductance catheter measurements during acute dynamic preload reductions in a porcine model (1). It was demonstrated that longitudinal strain inversely changed with EDV from
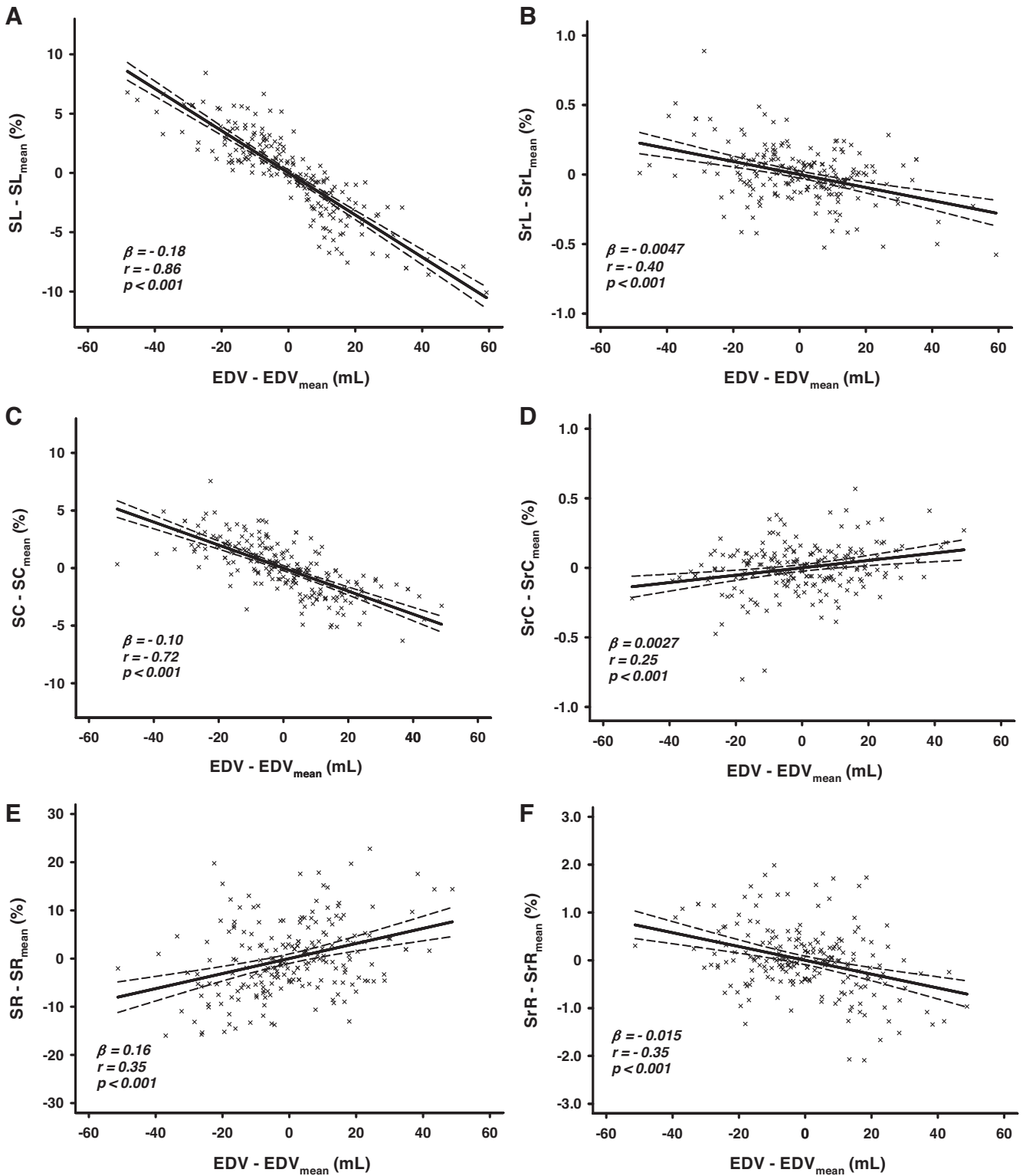
Fig. 2. Relative changes in speckle tracking strain (S; *A*, *C*, and *E*) and strain rate (Sr; *B*, *D*, and *F*) in the longitudinal (L), circumferential (C), and radial (R) direction of the left ventricle related to corresponding changes in end-diastolic volume (EDV) with linear regression and 95% confidence intervals. β, Slope of regression; *r*, regression coefficient; *p*, P value for regression.
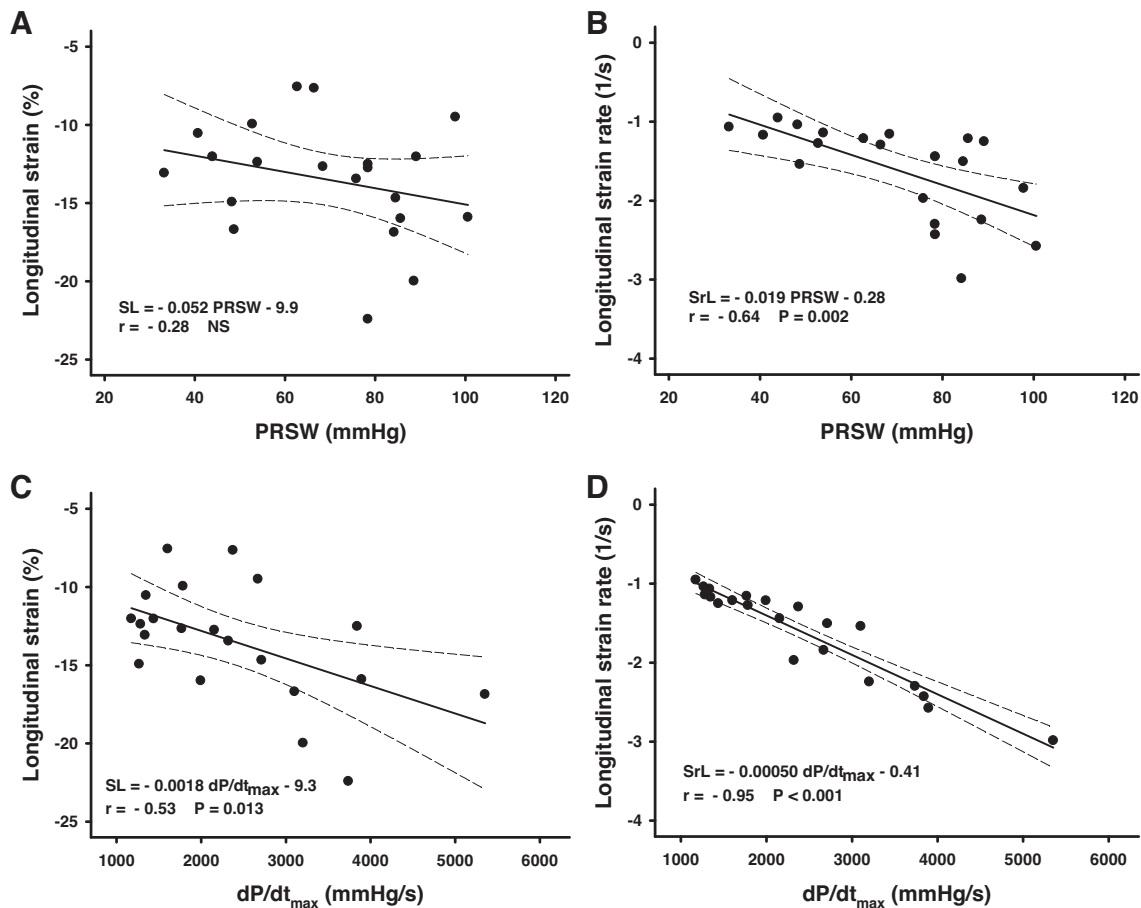
Fig. 3. Longitudinal strain (*A* and *C*) and strain rate (*B* and *D*) vs. preload recruitable stroke work (PRSW) and maximum of first derivative of left ventricular pressure (dP/dt_{max}) with corresponding regression lines and 95% confidence intervals. Regression functions with regression coefficients and *P* values.

baseline to β-adrenergic blockade; a finding in agreement with the present study. However, strain rate was not evaluated in the referred study.

Strain and strain rate as predictors of contractility. The slope of the PRSW was chosen as the main reference for inotropic state (14). In addition, it benefits from being independent of both the parallel conduction and the stroke volume calibrations when measured by the pressure-conductance catheter method. Also, it is based on the integration of pressure volume areas, which reduces noise artifacts. The LV-dP/dt_{max}, was also included as a reference for inotropic state as this parameter is widely used in experimental setups. Even though it is regarded less load independent compared with PRSW, it is recognized as a reasonably good estimate of left ventricular contractility (9). This parameter does not need acute load alteration to be obtained, and it also benefits from not incorporating volume estimates. In contrast to PRSW and dP/dt_{max}, all strain and strain rate parameters failed to differentiate baseline from the low dose of dobutamine (Table 1). However, strain rate could differentiate the Dob$_{high}$ from both baseline and Dob$_{low}$, whereas circumferential and radial strain differentiated Dob$_{high}$ from baseline, only. This demonstrates that strain rate is a more sensitive variable for describing inotropy. The weakest statistical correlation ($r = -0.58$), found for circumferential strain rate vs. PRSW, was highly significant (Fig. 4*B*). The low absolute value of the regression coefficient

($r = -0.010$) will, however, make this parameter susceptible to signal to noise errors. For the relationship between PRSW and longitudinal strain rate (Fig. 3*B*), the coefficient was more negative ($r = -0.019$), demonstrating more distinct alteration in strain rate with corresponding changes in PRSW. The strongest correlation ($r = 0.74$) and highest relative regression coefficient ($\beta = 0.048$) was found for radial strain rate vs. PRSW (Fig. 5*B*). A similar pattern was demonstrated for strain rates vs. LV-dP/dt_{max} in all echocardiographic planes. Thus radial strain rate is the most sensitive marker of contractility in our model. Neither circumferential nor longitudinal strain significantly correlates to PRSW. However, radial strain does correlate, indicating that it could be of some value as predictor of load-independent contractility.

Both clinical and experimental studies have shown that radial strain has poor reproducibility compared with especially longitudinal strain. Most of all, this is due to the limited time the speckles are present in a short-axis B-mode cineloop recording caused by in and out of plane motion, leading to small movements of speckles between two frames compared with a long-axis apical cineloop (8). However, the reproducibility for radial strain is also acceptable for clinical measurements although strain in the longitudinal direction is the most robust measure of myocardial strain in a clinical setting (4). Most important for reducing the errors in radial strain measurements are the frame rate, which must be high to follow the
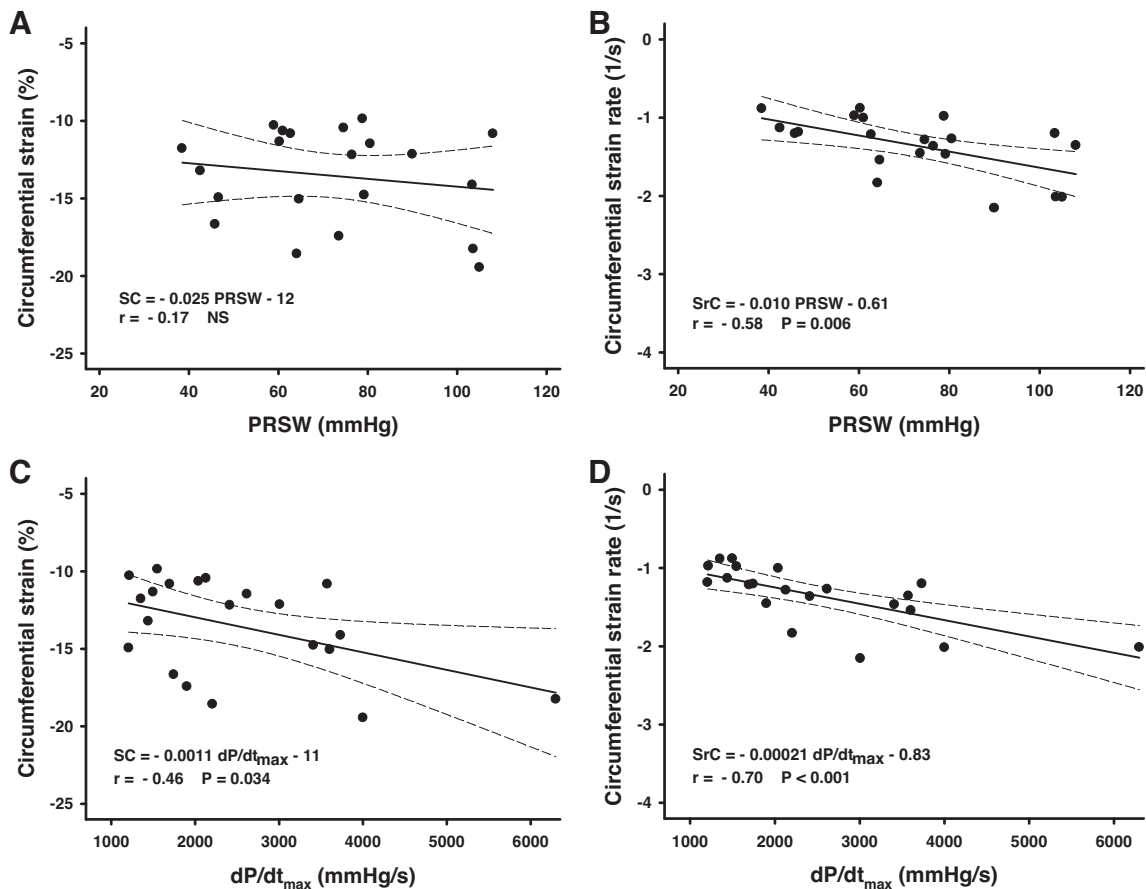
Fig. 4. Circumferential strain (*A* and *C*) and strain rate (*B* and *D*) vs. PRSW and maximum of first derivative of left ventricular pressure (dP/dt_{max}) with corresponding regression lines and 95% confidence intervals. Regression functions with regression coefficients and *P* values.

speckles in this direction. In this paper the frame rate was high for all measurements (103 ± 11 fps). This is also in accordance with the relative standard error of the mean being ~8–11% for radial strain, which is comparable to the respective values for circumferential and longitudinal strains (Table 1).

As expected, the coefficient of variations tends to be higher in the radial compared with circumferencial and longitudinal directions in the intra- and interobserver variability analysis. On the other, variation is relatively small and the intraclass correlation coefficients are excellent (Table 2).

From a three-dimensional chamber perspective, the radial direction is normal to both the circumferential and the longitudinal directions. Thus radial deformation is a function of the product of deformation in both the longitudinal and the circumferential directions, assuming conservation of myocardial volume. This relation could explain why the radial direction for both strain and strain rate is the most sensitive for contractile function and less dependent on geometry even though measurements in this direction is associated with more error.

Limitations. Temporal resolution is a concern when using speckle tracking of B-mode cineloops when calculating strain rate. The frame rate-to-heart rate ratio in this study was ~1 fps/bpm, which is acceptable according to recent studies (26–28). However, our results may not be valid for very high heart rates.

In this model we studied two-dimensional-derived strain and strain rate in different directions and compared them to left-

ventricular EDV and contractility parameters acquired by the conductance catheter. We have averaged all segments from the speckle tracking analysis from each recording. The use of 16 segments from three apical views for calculation of global longitudinal strain would provide a more accurate estimate of global longitudinal strain. However, to avoid excessive preload reductions only one four-chamber view and one mid-ventricular short-axis view have been investigated in each situation. Three-dimensional echocardiography could give an even more complete picture and a better estimate of global strain. However, stitching techniques cannot be used in this model as ventricular filling is different from one beat to the next, thus severely limiting temporal and spatial resolution.

Random noise and in-and-out of plane motion lead to inaccuracies in the tracking of speckles. This will cause the estimated speckle positions to drift through the cardiac cycle. The algorithm therefore has an incorporated drift compensation, which assumes that speckles should resume their original position at the end of each cycle. Deviation from this introduces drift of the strain estimate. In our study, this assumption is a priori violated as we reduce the filling from one beat to the next. However, only minimal differences were seen when toggling drift compensation, except in a few special cases where acoustic artifacts made acceptable tracking impossible when drift compensation was turned off.

In addition to changes in contractile function, chronotropy, and loading conditions, strain and strain rate are correlated to
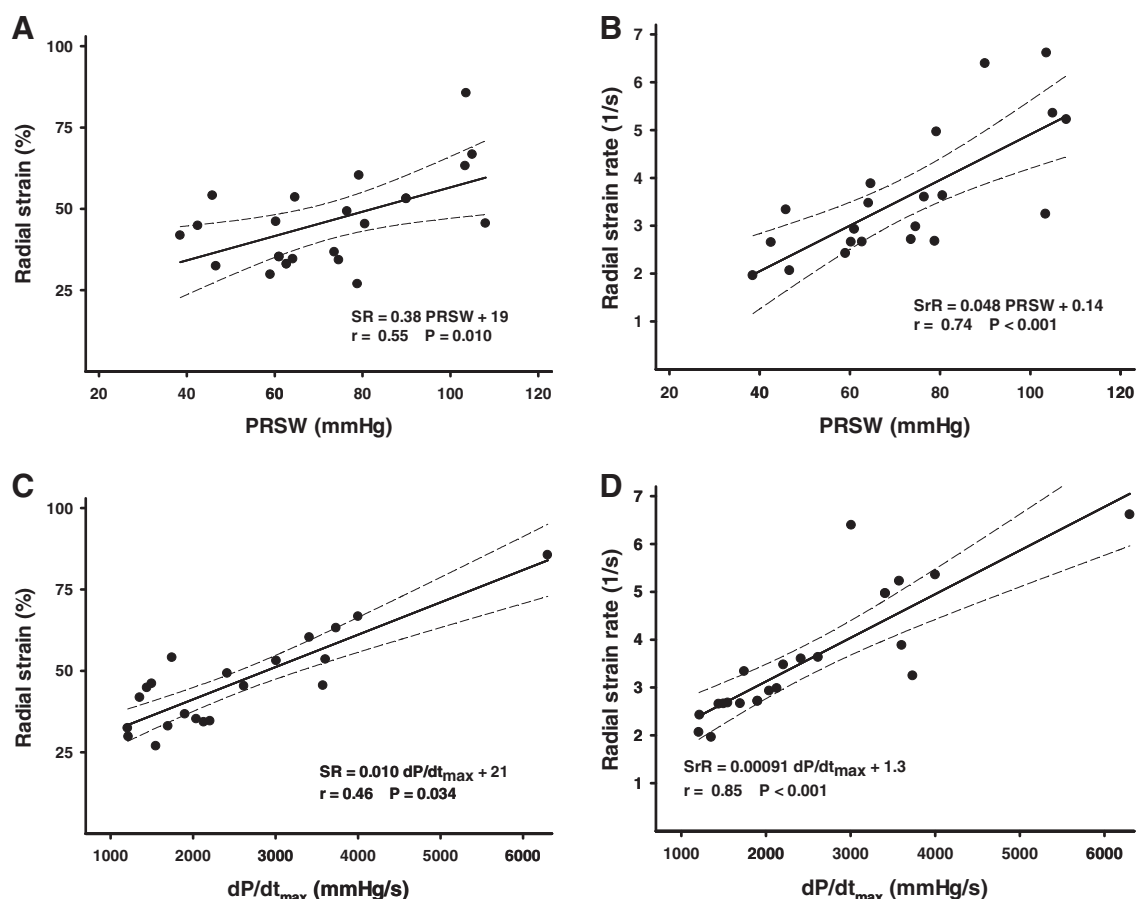
Fig. 5. Radial strain (*A* and *C*) and strain rate (*B* and *D*) vs. PRSW and maximum of first derivative of left ventricular pressure (dP/dt_{max}) with corresponding regression lines and 95% confidence intervals. Regression functions with regression coefficients and *P* values.

body weight and myocardial size and geometry. For the pig, a convincing hyperbolic relation between body weight and longitudinal strain and strain rate has been demonstrated (24). In the present study, we have minimized the influence of this relationship as we have kept the range of body weights narrow (39–45 kg). Caution should therefore be taken in comparison of data from groups with large distribution in body weight. Furthermore, the sensitivity to load changes in the three directions could differ for various pathophysiological states compared with the heathly hearts studied here.

Table 2. *ICC and CV for inter- and intraobserver variability for global strain and strain rate evaluated by speckle tracking in the circumferential, radial, and longitudinal direction of the left ventricle*

Variable	Interobserver (n = 20)		Intraobserver (n = 20)	
	ICC	CV, %	ICC	CV, %
SC	0.885	8.31	0.870	9.19
SrC	0.937	8.14	0.900	11.97
SR	0.913	11.18	0.925	9.85
SrR	0.895	14.78	0.903	15.10
SL	0.920	8.71	0.891	11.22
SrL	0.958	8.09	0.957	8.18

ICC, Interclass correlation coefficient; CV, coefficient of variation; S, strain; Sr, strain rate; C, R, L, circumferential, radial, and longitudinal directions.

During the unloading both preload and afterload will alter. However, since the caval occlusion systematically restraints the filling, the EDV was used as the loading marker. This parallels with the PRSW, the slope between stroke work vs. EDV. We emphasize that we have not attempted to separate the pre- and afterload, and covariations in afterload probably have a significant influence on the correlations between EDV and strain. As such, the results between the deformation analysis and unloading are thus strictly valid only for caval occlusions.

The anterio-posterior orientation of the pig heart makes apical long-axis images almost unobtainable by transthoracal echocardiography. In addition, the narrow intercostal spaces combined with lungs overlapping the heart limit the short-axis image quality (17). The porcine anatomy is also reported to hinder complete short-axis images with the transesophageal approach (23). To avoid this, optimized image quality was obtained through a gel-filled acoustic window created by surgically resection of the lower sternal chest wall. The pleura and pericardium were kept intact to limit change in positional restraint. Beat to beat variations caused by positive pressure ventilation were avoided by obtaining all recordings during respirator shut-off at zero expiratory pressure.

With dobutamine infusions, the left ventricular-ejection fraction did not change despite an observed increase in cardiac index. This is explained by the increased heart rate without changes in stroke volume. EDVs did not change. Conse-

quently, the unaltered left ventricular-ejection fraction supports its load dependency. Alternatively, errors in absolute volume estimates introduced by calibration of the conductance catheter could also explain the unaltered left ventricular-ejection fraction. Also, the statistical power in the present study is low, and negative findings should be interpreted with caution.

Conclusion. This study demonstrates that both strain and strain rate assessed by speckle tracking echocardiography are sensitive to acute dynamic unloading by caval occlusion maneuvers. However, strain and strain rate in different directions were affected to a variable degree in this model. Strain rate in the radial direction is the most sensitive parameter for changes in contractility and the least sensitive to unloading. Thus radial strain rate is preferable when evaluating inotropic function. Longitudinal and circumferential strain on the other hand is vulnerable to acute loading differences and should not be used as a direct contractility measurement.

DISCLOSURES

No conflicts of interest, financial or otherwise, are declared by the author(s).

AUTHOR CONTRIBUTIONS

Author contributions: G.O.D., L.S., C.A.M., P.-R.S., K.M., and K.G. conception and design of research; G.O.D., L.S., C.A.M., P.-R.S., K.M., and K.G. performed experiments; G.O.D., K.M., and K.G. analyzed data; G.O.D., C.A.M., R.H., K.M., and K.G. interpreted results of experiments; G.O.D., K.M., and K.G. prepared figures; G.O.D., C.A.M., K.M., and K.G. drafted manuscript; G.O.D., L.S., C.A.M., P.-R.S., R.H., K.M., and K.G. edited and revised manuscript; G.O.D., L.S., C.A.M., P.-R.S., R.H., K.M., and K.G. approved final version of manuscript.

REFERENCES

1. **A'Roch R, Gustafsson U, Johansson G, Poelaert J, Haney M.** Left ventricular strain and peak systolic velocity: responses to controlled changes in load and contractility, explored in a porcine model. *Cardiovasc Ultrasound* 10: 22, 2012.
2. **Abraham TP, Laskowski C, Zhan WZ, Belohlavek M, Martin EA, Greenleaf JF, Sieck GC.** Myocardial contractility by strain echocardiography: comparison with physiological measurements in an in vitro model. *Am J Physiol Heart Circ Physiol* 285: H2599–H2604, 2003.
3. **Andersen NH, Terkelsen CJ, Sloth E, Poulsen SH.** Influence of preload alterations on parameters of systolic left ventricular long-axis function: a Doppler tissue study. *J Am Soc Echocardiogr* 17: 941–947, 2004.
4. **Armstrong AC, Ricketts EP, Cox C, Adler P, Arynchyn A, Liu K, Stengel E, Sidney S, Lewis CE, Schreiner PJ, Shikany JM, Keck K, Merlo J, Gidding SS, Lima JA.** Quality control and reproducibility in M-mode, two-dimensional, and speckle tracking echocardiography acquisition and analysis: The CARDIA Study, Year 25 Examination Experience. *Echocardiography* 32: 1233–1240, 2015.
5. **Baan J, van der Velde ET, de Bruin HG, Smeenk GJ, Koops J, van Dijk AD, Temmerman D, Senden J, Buis B.** Continuous measurement of left ventricular volume in animals and humans by conductance catheter. *Circulation* 70: 812–823, 1984.
6. **Burkhoff D, Mirsky I, Suga H.** Assessment of systolic and diastolic ventricular properties via pressure-volume analysis: a guide for clinical, translational, and basic researchers. *Am J Physiol Heart Circ Physiol* 289: H501–H512, 2005.
7. **Burns AT, La Gerche A, D'Hooge J, MacIsaac AI, Prior DL.** Left ventricular strain and strain rate: characterization of the effect of load in human subjects. *Eur J Echocardiogr* 11: 283–289, 2010.
8. **Cameli M, Mondillo S, Solari M, Righini FM, Andrei V, Contaldi C, De Marco E, Di Mauro M, Esposito R, Gallina S, Montisci R, Rossi A, Galderisi M, Nistri S, Agricola E, Mele D.** Echocardiographic assessment of left ventricular systolic function: from ejection fraction to torsion. *Heart Fail Rev* 21: 77–94, 2016.
9. **Carabello BA.** Evolution of the study of left ventricular function: everything old is new again. *Circulation* 105: 2701–2703, 2002.
10. **Cingolani HE, Pérez NG, Cingolani OH, Ennis IL.** The Anrep effect: 100 years later. *Am J Physiol Heart Circ Physiol* 304: H175–H182, 2013.
11. **Edvardsen T, Haugaa KH.** Imaging assessment of ventricular mechanics. *Heart* 97: 1349–1356, 2011.
12. **Fanneløp T, Dahle GO, Matre K, Segadal L, Grong K.** An anaesthetic protocol in the young domestic pig allowing neuromuscular blockade for studies of cardiac function following cardioplegic arrest and cardiopulmonary bypass. *Acta Anaesthesiol Scand* 48: 1144–1154, 2004.
13. **Ferferieva V, Van den Bergh A, Claus P, Jasaityte R, Veulemans P, Pellens M, La Gerche A, Rademakers F, Herijgers P, D'Hooge J.** The relative value of strain and strain rate for defining intrinsic myocardial function. *Am J Physiol Heart Circ Physiol* 302: H188–H195, 2012.
14. **Glower DD, Spratt JA, Snow ND, Kabas JS, Davis JW, Olsen CO, Tyson GS, Sabiston DC, Rankin JS.** Linearity of the Frank-Starling relationship in the intact heart: the concept of preload recruitable stroke work. *Circulation* 71: 994–1009, 1985.
15. **Grong K, Salminen PR, Stangeland L, Dahle GO.** Haemodynamic differences between pancuronium and vecuronium in an experimental pig model. *Vet Anaesth Analg* 42: 242–249, 2015.
16. **Hawk CT, Leary SL, Morris TH, American College of Laboratory Animal Medicine, European College of Laboratory Animal Medicine.** *Formulary for Laboratory Animals.* Ames, IA: Blackwell, 2005.
17. **Kerut EK, Valina CM, Luka T, Pinkernell K, Delafontaine P, Alt EU.** Technique and imaging for transthoracic echocardiography of the laboratory pig. *Echocardiography* 21: 439–442, 2004.
18. **Kovacs A, Olah A, Lux A, Matyas C, Nemeth BT, Kellermayer D, Ruppert M, Torok M, Szabo L, Meltzer A, Assabiny A, Birtalan E, Merkely B, Radovits T.** Strain and strain rate by speckle-tracking echocardiography correlate with pressure-volume loop-derived contractility indices in a rat model of athlete's heart. *Am J Physiol Heart Circ Physiol* 308: H743–H748, 2015.
19. **Lakatta EG.** Beyond Bowditch: the convergence of cardiac chronotropy and inotropy. *Cell Calcium* 35: 629–642, 2004.
20. **Lang RM, Badano LP, Mor-Avi V, Afilalo J, Armstrong A, Ernande L, Flachskampf FA, Foster E, Goldstein SA, Kuznetsova T, Lancellotti P, Muraru D, Picard MH, Rietzschel ER, Rudski L, Spencer KT, Tsang W, Voigt JU.** Recommendations for cardiac chamber quantification by echocardiography in adults: an update from the American Society of Echocardiography and the European Association of Cardiovascular Imaging. *Eur Heart J Cardiovasc Imaging* 16: 233–270, 2015.
21. **Moen CA, Salminen PR, Dahle GO, Hjertaas JJ, Grong K, Matre K.** Is strain by speckle tracking echocardiography dependent on user controlled spatial and temporal smoothing? An experimental porcine study. *Cardiovasc Ultrasound* 11: 32, 2013.
22. **Raff GL, Glantz SA.** Volume loading slows left ventricular isovolumic relaxation rate. Evidence of load-dependent relaxation in the intact dog heart. *Circ Res* 48: 813–824, 1981.
23. **Ren JF, Schwartzman D, Lighty GW Jr, Menz VV, Michele JJ, Li KS, Dillon SM, Marchlinski FE, Segal BL.** Multiplane transesophageal and intracardiac echocardiography in large swine: imaging technique, normal values, and research applications. *Echocardiography* 14: 135–148, 1997.
24. **Rosner A, Bijnens B, Hansen M, How OJ, Aarsaether E, Muller S, Sutherland GR, Myrmel T.** Left ventricular size determines tissue Doppler-derived longitudinal strain and strain rate. *Eur J Echocardiogr* 10: 271–277, 2009.
25. **Royse CF, Connelly KA, MacLaren G, Royse AG.** Evaluation of echocardiography indices of systolic function: a comparative study using pressure-volume loops in patients undergoing coronary artery bypass surgery. *Anaesthesia* 62: 109–116, 2007.
26. **Rösner A, Barbosa D, Aarsæther E, Kjønås D, Schirmer H, D'hooge J.** The influence of frame rate on two-dimensional speckle-tracking strain

measurements: a study on silico-simulated models and images recorded in patients. *Eur Heart J Cardiovasc Imaging*, 2015.

27. **Sanchez AA, Levy PT, Sekarski TJ, Hamvas A, Holland MR, Singh GK.** Effects of frame rate on two-dimensional speckle tracking-derived measurements of myocardial deformation in premature infants. *Echocardiography* 32: 839–847, 2015.

28. **Singh GK, Cupps B, Pasque M, Woodard PK, Holland MR, Ludomirsky A.** Accuracy and reproducibility of strain by speckle tracking in pediatric subjects with normal heart and single ventricular physiology: a two-dimensional speckle-tracking echocardiography and magnetic resonance imaging correlative study. *J Am Soc Echocardiogr* 23: 1143–1152, 2010.

29. **Sutherland GR, Di Salvo G, Claus P, D'hooge J, Bijnens B.** Strain and strain rate imaging: a new clinical approach to quantifying regional myocardial function. *J Am Soc Echocardiogr* 17: 788–802, 2004.

30. **Urheim S, Edvardsen T, Torp H, Angelsen B, Smiseth OA.** Myocardial strain by Doppler echocardiography. Validation of a new method to quantify regional myocardial function. *Circulation* 102: 1158–1164, 2000.

31. **Yotti R, Bermejo J, Benito Y, Sanz-Ruiz R, Ripoll C, Martínez-Legazpi P, del Villar CP, Elízaga J, González-Mansilla A, Barrio A, Bañares R, Fernández-Avilés F.** Validation of noninvasive indices of global systolic function in patients with normal and abnormal loading conditions: a simultaneous echocardiography pressure-volume catheterization study. *Circ Cardiovasc Imaging* 7: 164–172, 2014.